

Article

Effect of Water-Air Microemulsion of Flotation Agent Solution on Flotation of Polymetallic Sulfide Ores

Dulatbek Turysbekov , Nessipbay Tussupbayev, Sabira Narbekova *  and Zhamikhan Kaldybayeva

Institute of Metallurgy and Ore Beneficiation JSC, Satbayev University, Almaty 050010, Kazakhstan

* Correspondence: s.narbekova@mail.ru

Abstract: The enrichment of polymetallic sulfide ore is a complex task. Fine grinding is carried out to reveal useful minerals, resulting in the formation of microparticles. It is difficult to achieve the flotation of microparticles and fine useful minerals are lost with flotation tailings. The problem of microparticle flotation can be solved by using air bubbles smaller than 50 μm for the flotation process. Water-air microemulsion (WAME) of a frothersolution obtained using the generator was used as microbubbles. The effect of WAME on flotation was studied on polymetallic ores and gold-bearing ore from Kazakhstan deposits. The use of WAME in the processing of polymetallic ore allowed for the maintenance of the quality of rougher concentrates, to increase the copper extraction in Cu-Pb rougher concentrate by 7.41%, of lead by 5.98% in the copper-lead flotation cycle (Cu-Pb-Zn-Fe ore), copper extraction in Cu-Mo rougher concentrate by 5.2%, and molybdenum by 4.7% in the copper-molybdenum flotation cycle (Cu-Mo ore). The indicators of flotation gold extraction into the gold-containing concentrate significantly improved in comparison with the basic mode when using the generator in rougher and scavenger flotation cycles: the quality increased by 5.3 g/t, and the extraction increased by 4.27%.

Keywords: flotation; fine particle; microbubbles; water-air microemulsion; rougher flotation; frother



Citation: Turysbekov, D.; Tussupbayev, N.; Narbekova, S.; Kaldybayeva, Z. Effect of Water-Air Microemulsion of Flotation Agent Solution on Flotation of Polymetallic Sulfide Ores. *Minerals* **2022**, *12*, 1612. <https://doi.org/10.3390/min12121612>

Academic Editor: George Blankson Abaka-Wood

Received: 28 October 2022
Accepted: 12 December 2022
Published: 14 December 2022

Publisher's Note: MDPI stays neutral with regard to jurisdictional claims in published maps and institutional affiliations.



Copyright: © 2022 by the authors. Licensee MDPI, Basel, Switzerland. This article is an open access article distributed under the terms and conditions of the Creative Commons Attribution (CC BY) license (<https://creativecommons.org/licenses/by/4.0/>).

1. Introduction

The flotation of fine particles smaller than 50 μm is a challenge for the mining industry [1,2]. At present, most of the processed ores in Kazakhstan are characterized by the close intergrowth of very thin, approaching colloidal, mineral inclusions. The mineral grains containing useful components are so small that the entire ore must be finely crushed in order to dissect them, isolate them into free particles and separate them from the host rock. The optimal grain size for flotation enrichment is $\sim 70 \mu\text{m}$, but a significant part of the currently mined ores requires much deeper grinding down to 30–40 μm . Because of this, a significant part of the uncovered monomineral grains containing useful metals is lost with microdispersions (super-slimes). If the microparticles of useful minerals have insignificant mass, they cannot accumulate kinetic energy in motion and overcome the water-structural energy barrier to connect with air bubbles. As a consequence, the non-ferrous metal extraction decreases from 50 to 30%, both at the selective and rougher flotation.

In the middle of the last century, the most effective method of microparticle enrichment was flotation, with many studies using aeration by gases released from aqueous solutions [3–7]. The problem can be solved by the use of combined microflotation, where both micro- and macrobubbles participate in the flotation process [8–10].

The problem of microparticle flotation can be solved by using air bubbles smaller than 50 μm in the flotation process [11,12]. There are various ways to produce microbubbles [13,14] and nanobubbles [15,16]. The fundamentally new method, “turbulent microflotation”, was developed, since the use of very small bubbles in the currently used flotation machines is associated with some technological difficulties [17,18]. The essence of this method is that small air bubbles are formed outside the processed pulp. Microbubbles

in the form of the concentrated water-air microemulsion are formed in the generator, then mixed with the pulp and passed through a tubular static mixer (flotation reactor) as a turbulent flow. As a result, the microbubbles are mineralized in the flotation reactor; they enlarge due to coalescence and aggregate into large flotation complexes containing thousands of initial microbubbles, and this contributes to the rapid separation of pulp by sedimentation.

Bubbles of different sizes are present simultaneously in the flotation system when using water-air microemulsion: microbubbles of 20–70 microns, medium bubbles due to the connection of several microbubbles, and macrobubbles generated by the flotation machine aerator. Microbubble and bubble cascades are mobile, more floactive, attract to themselves fine minerals smaller than 30 microns, and adhere to the macrobubble surface, floating to the pulp surface in the flotation concentrate form [1]. The use of a water-air microemulsion frother solution intensifies the process of microparticle flotation. The purpose of this research is to study the effect of water-air microemulsion produced in a generator on the flotation ability of sulfide minerals of non-ferrous metals and gold. This work's novelty is to determine the generator operating parameters, to choose the optimal concentration of reagent solutions in order to obtain a water-air microemulsion of the required amount to extract valuable mineral microparticles, and to study the effect of the WAME generator on sulfide ore flotation.

2. Experimental Section

2.1. Polymetallic Ores Samples

2.1.1. Polymetallic Cu-Pb-Zn-Fe Ore Sample

A sample of Cu-Pb-Zn-Fe polymetallic ore was used for the flotation experiments. The chemical composition of the initial ore sample was: Cu 0.42%; Pb 0.52%; Zn 3.11%; Fe 6.21%; S 8.2%; Al₂O₃ 7.74%; SiO₂ 54.0%; CaO 2.24%; MgO 8.38%. The sample contained 1.0 g/t gold, and 8.8 g/t silver. The main useful components in the ore were copper, lead, and zinc. Gold is mainly associated with sulfides, especially closely associated with pyrite.

The ore contained chalcopyrite CuFeS₂, pyrite FeS₂, galena PbS, sphalerite ZnS, quartz α -SiO₂, calcite CaCO₃, talcum Mg₃Si₄O₁₀(OH)₄, chrysotile Mg₆Si₄O₁₀(OH)₈, albite NaAlSi₃O₈, and muscovite KAl₂Si₃AlO₁₀(OH)₂, which was confirmed by X-ray diffraction analysis. The X-ray phase analysis of the sample was performed on a D8 Advance (Bruker, Billerica, MA, USA), α -Cu, 40/40 tube voltage. Diffractogram decoding and interplanar distance calculation were performed using EVA software (Bruker, Billerica, MA, USA). The granulometric composition of the crushed Cu-Pb-Zn-Fe polymetallic ore is shown in Table 1.

Table 1. Granulometric composition of crushed Cu-Pb-Zn-Fe polymetallic ore.

Size Class, μm	Yield, %	Content, %				Distribution, %			
		Cu	Pb	Zn	Fe	Cu	Pb	Zn	Fe
+74	13	0.38	0.52	3.01	5.99	11.79	13.47	9.81	12.64
−74 + 50	15	0.41	0.61	3.81	6.74	14.68	18.24	14.33	16.41
−50 + 40	18	0.5	0.54	5.01	5.88	21.48	19.37	22.61	17.18
−40 + 30	13	0.39	0.47	3.45	6.35	12.10	12.18	11.25	13.40
−30 + 20	17	0.38	0.39	4.22	6.01	15.42	13.22	17.99	16.58
−20 + 10	14	0.47	0.55	3.93	7.0	15.70	15.35	13.80	15.91
−10 + 0	10	0.37	0.41	4.07	4.86	8.83	8.17	10.21	7.89
Initial product	100	0.42	0.50	3.99	6.16	100.0	100.0	100.0	100.0

Particle size analysis of the crushed ore showed that 87.0% of the useful minerals were concentrated in the fraction -0.074 mm.

2.1.2. Polymetallic Cu-Mo Ore Sample

The ore contained copper and molybdenum. Associated components were sulfur, lead, and zinc. The main minerals were chalcopyrite, bornite, and chalcocite. The copper content varied in ores, from 0.2 to 1.6%, and the average content was 0.39%.

The chemical analysis of the ore sample showed the following concentrations of minerals: 0.009% molybdenum; 0.4% copper; 0.58% sulfur; 5.2% iron; 4.6% CaO; 16.5% Al₂O₃; 55.7% SiO₂; 4.6% MgO; 0.27% Ti.

Chalcopyrite is the main copper-bearing mineral. It is characterized by a relatively uniform distribution. Inclusions sized 0.003–1.0 mm are its characteristic form. In enriched areas, chalcopyrite forms nests and clusters of 1.8–2.5 mm. Molybdenite forms single plates (0.001–0.1 mm) in quartz, chlorite-quartz-calicheptic, and calicheptic veins.

X-ray phase analysis showed that the ore contained quartz SiO₂, albite (Na,Ca)Al(Si,Al)₃O₈, anorthite (Ca,Na)(Si,Al)₄O₈, clinoclone Mg₅Al(Si₃Al)O₁₀(OH)₈, nepheline (K,Na)AlSiO₄, and muscovite KAl₂Si₃AlO₁₀(OH)₂. The granulometric composition of the crushed Cu-Mo polymetallic ore is shown in Table 2.

Table 2. Granulometric composition of crushed Cu-Mo polymetallic ore.

Size Class, μm	Yield, %	Content, %		Distribution, %	
		Cu	Mo	Cu	Mo
−74 + 60	19.9	0.41	0.017	21.2	30.9
−60 + 50	12.3	0.37	0.009	11.8	10.1
−50 + 40	12.3	0.38	0.011	12.1	12.3
−40 + 30	2.0	0.43	0.011	2.3	2.0
−30 + 20	10.7	0.38	0.009	10.5	8.7
−20 + 10	23.6	0.39	0.011	23.8	23.7
−10 + 0	19.2	0.37	0.007	18.3	12.3
Initial product	100	0.39	0.011	100.0	100.0

2.1.3. Gold-Bearing Ore Sample

The material composition of the sample was quartz-coated diorites with arsenopyrite-free gold mineralization. The average gold content in the studied sample is 2.4 g/t.

The chemical analysis of the ore sample revealed the following mineral concentrations: SiO₂ 62.44%, Al₂O₃ 15.0%, CaO 3.56%, MgO 1.18%, Fe_{total} 4.44%, S_{total} 0.48%, Cu 0.01%, Pb 0.02%, Zn 0.01%, As 1.0%.

X-ray phase analysis showed that the ore contained quartz, clinoclone Mg_{2.5}Fe_{1.65}Al_{1.5}Si_{2.2}Al_{1.8}O₁₀(OH)₈, muscovite KAl₂Si₃AlO₁₀(OH)₂, albite Na(AlSi₃O₈), and aluminian (Mg_{0.944}Fe_{0.056})(Ca_{0.844}Na_{0.142}Fe_{0.014})(Si_{1.86}Al_{0.14}O₆).

The rational composition of gold in a sample of gold-bearing ore is presented in Table 3.

Table 3. Rational composition of gold in the ore sample.

Gold Association Form	Content, g/t	Distribution, %
Fine-grained native gold	0.58	22.14
Visible native gold	0.84	32.06
In aggregates with sulfides and rock	0.24	9.16
Associated with sulfides	0.48	18.32
Associated with the rock	0.27	10.31
In quartz	0.21	8.02
Total	2.62	100.0

The granulometric composition of the crushed gold-bearing ore is shown in Table 4.

Table 4. Granulometric composition of crushed gold-bearing ore.

Size Class, μm	Yield, %	Content, %	Distribution, %
−1.0	20.76	0.8	6.92
−1.0 + 0.5	15.17	4.0	25.30
−0.5 + 0.4	14.99	1.5	9.37
− 0.4 + 0.2	6.04	3.2	8.06
−0.2 + 0.1	9.82	3.8	15.56
−0.1 + 0.074	26.20	2.3	25.12
−0.074 + 0	7.02	3.3	9.66
Total	100	2.40	100

2.2. Schemes and Reagent Regimes of Ore Flotation

2.2.1. Scheme and Reagent Mode of Cu-Pb-Zn-Fe Ore Flotation

Flotation experiments were carried out on laboratory flotation machines FML-1 and FML-2. The ore weighting for the experiment was 500 g. The flotation scheme included a cycle of rougher flotation from which copper-lead concentrate was obtained and two cleaner flotations of rougher concentrate. The scheme is presented in Figure 1.

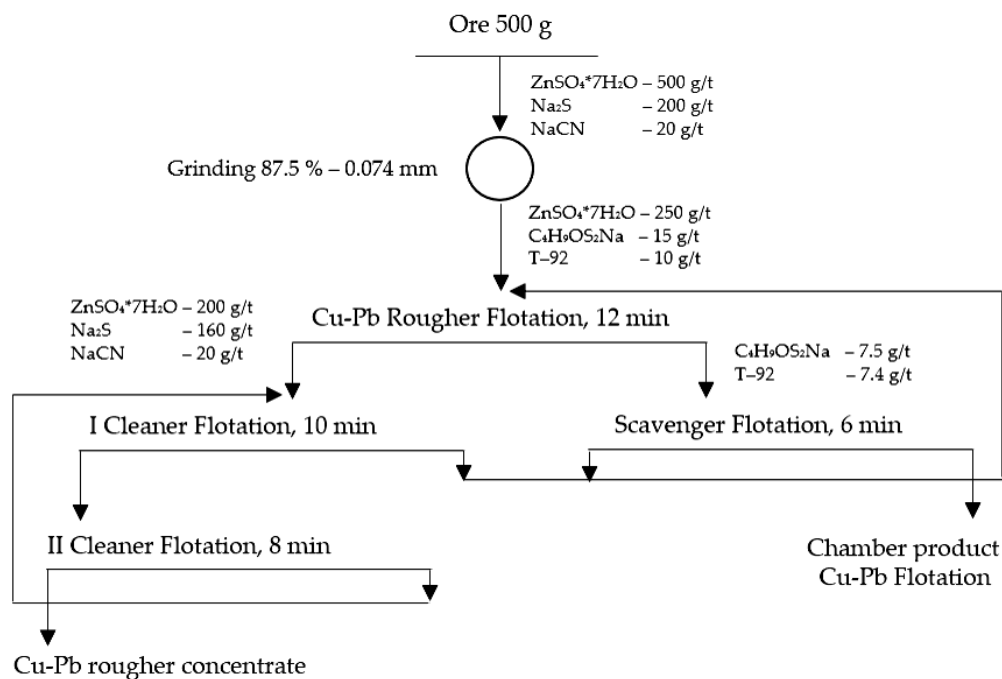


Figure 1. Scheme of copper-lead rougher flotation of ore.

Rougher flotation was carried out at pH 8.0–9.0. The reagent mode of rougher flotation was: sodium sulfide was fed into the grinding process for mineral sulfidization; zinc sulfate and sodium cyanide were used for depression of zinc and iron sulfide minerals; sodium butyl xanthogenate was used as a collector; and oxal T-92 was used as frother. The rougher flotation time was 12 min. The collector and frother were fed fractionally in several portions into the rougher flotation. Additionally, sulfate and sodium cyanide were fed into the cleaner flotations, and the rougher concentrate was purified of zinc and iron minerals to obtain a higher-quality rougher concentrate. The collector and frother were fed into the scavenger flotation for the additional extraction of lead and copper minerals.

2.2.2. Scheme and Reagent Mode of Cu-Mo Ore Flotation

The flotation scheme included a cycle of rougher flotation to produce a copper-molybdenum concentrate and three cleaner flotation cycles of the rougher concentrate. Lime was fed in during the grinding process to achieve a pH of 8.0–9.0, along with sodium sulfide to sulfidize the minerals. The time of the copper-molybdenum rougher flotation was 16 min, and the time of the scavenger flotation was 7 min. Sodium butyl xanthogenate was used as a collector; T-92 was used as a frother. The liquid glass was fed into the cleaner flotation to depress the waste rock minerals. The scheme and reagent base mode are shown in Figure 2.

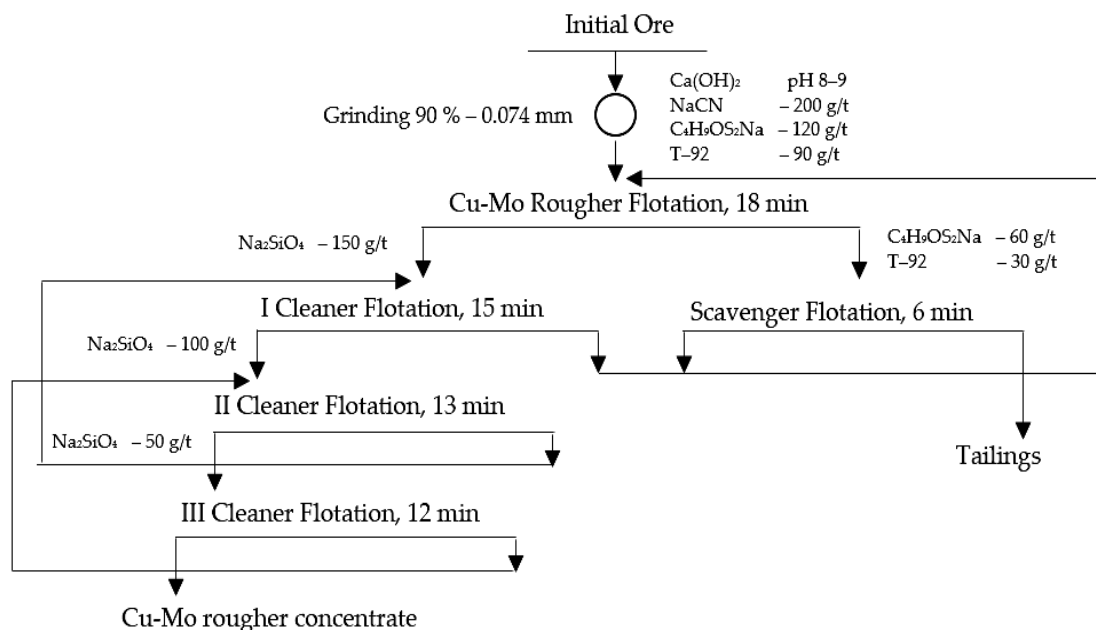


Figure 2. Scheme of copper-molybdenum rougher flotation of ore.

2.2.3. Scheme and Reagent Mode of Gold-Bearing Ore Flotation

The scheme of the flotation included inter-cycle, rougher, and scavenger flotations and cleaner flotations of the rougher product (Figure 3).

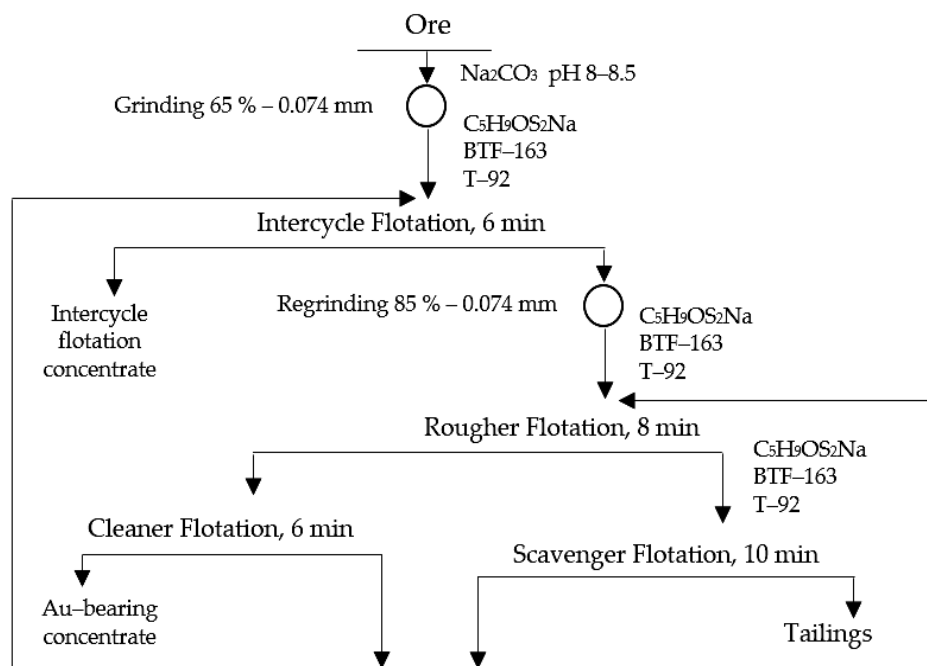


Figure 3. Scheme of gold-bearing ore flotation.

Lime was fed in during the grinding process to achieve a pH of 8.0–8.5. The experiments were carried out on five 1000 g portions of ore. According to the basic mode, the total amount of reagents was: sodium butyl xanthate $C_5H_9OS_2Na$ —96 g/t; BTF-163—24 g/t; T-92—17 g/t. When using a WAME generator, the reagent amount was: sodium butyl xanthate—96 g/t; BTF-163—24 g/t; T-92—8.5 g/t.

2.3. Water-Air Microdispersion Generator and Operating Parameters

The installation of the WAME generator is shown in Figure 4.

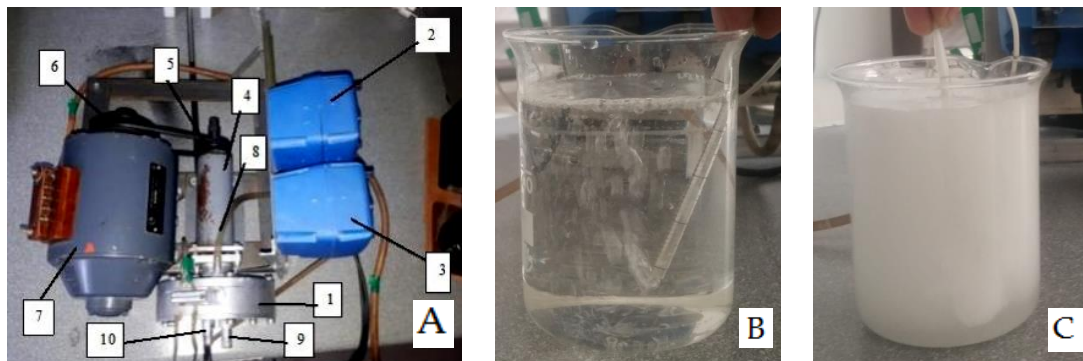


Figure 4. (A) Water-air microemulsion generator. (B) Image of frother solution before dispersion. (C) Image of frother solution after dispersion in the generator. (A) WAME generator: 1—dispersing chamber; 2—air pump; 3—frother solution pump; 4—gearbox; 5—gearbox pulley; 6—electric motor pulley; 7—electric motor; 8—input for air and frother solution in generator; 9—outlet for cooling water; 10—input for cooling water.

The operation principle of the laboratory generator is that, through the metering pumps, air and frother solution enter through the inlet pipe into the dispersion chamber. There is an additional mixing of the mixture with the dispersion chamber rotor. Due to the high peripheral speed, the mixture is thrown to the periphery and passes through the slot between the rotor and the stator. The size of the slot between the stator and rotor is determined by the raw material composition and the required crushing degree. The rotor protrusions crush the air bubbles into microbubbles as the rotor rotates. The output is a water-air microemulsion, the size and stability of which depend on many factors: on the solution concentration, the frother type, and the speed of generator rotation.

Optimal generator parameters: generator speed 6000 rpm; liquid:gas phase ratio $L:G = 1:1$; the dosing pump capacity $6\text{--}7.2\text{ dm}^3/\text{min}$ [19,20]. The optimal pulp temperature during flotation, which preserves the microemulsion stability, is $20\text{--}40\text{ }^\circ\text{C}$ [19].

2.4. Effect of Frother Solution Concentration on Stability and Size of WAME

The effect of the flotation agent concentration on the stability and size of the WAME obtained from T-92 and sodium salt of dibutyl dithiophosphoric acid BTF-163 was studied. The reagent concentration varied from 0.05 to 50 g/dm^3 . The measurement temperature ranged from $20\text{ }^\circ\text{C}$ to $40\text{ }^\circ\text{C}$. The size of WAME was determined using a particle size analyzer SALD-2101 (Shimadzu, Kyoto, Japan).

The reagent solution's electrokinetic potential was measured on a Photocor Compact (Photocor Ltd., Moscow, Russia). The adsorption of reagents was associated with a change in the surface tension of the reagent solution at the liquid–air interface. The analysis of the frother solution's surface tension at various concentrations (solution pH was 8.5–9) was performed with a tensiometer, K20 EasyDyne series (KRUS, Hamburg, Germany).

2.5. Frother Solution Foaming Ability

Reagent foamability was determined as follows. From the initial frother solution, solutions of different concentrations were prepared, and then they were frothed. To

do this, about 10–12 mL of frother solution was poured into the foam generator, which was connected to a microcompressor and barbotaged through a solution of pre-cleaned and humidified air. When a certain volume of foam was reached, the air supply was stopped. The measurements of the foam volume and the liquid in the foam were carried out every 15–20 s.

3. Results and Discussion

3.1. Effect of Frother Solution Concentration on Stability and Size of WAME

Figure 5 shows the results of the effect of the concentration of the reagent solution on the stability and size of the WAME at a generator speed of 6000 rpm.

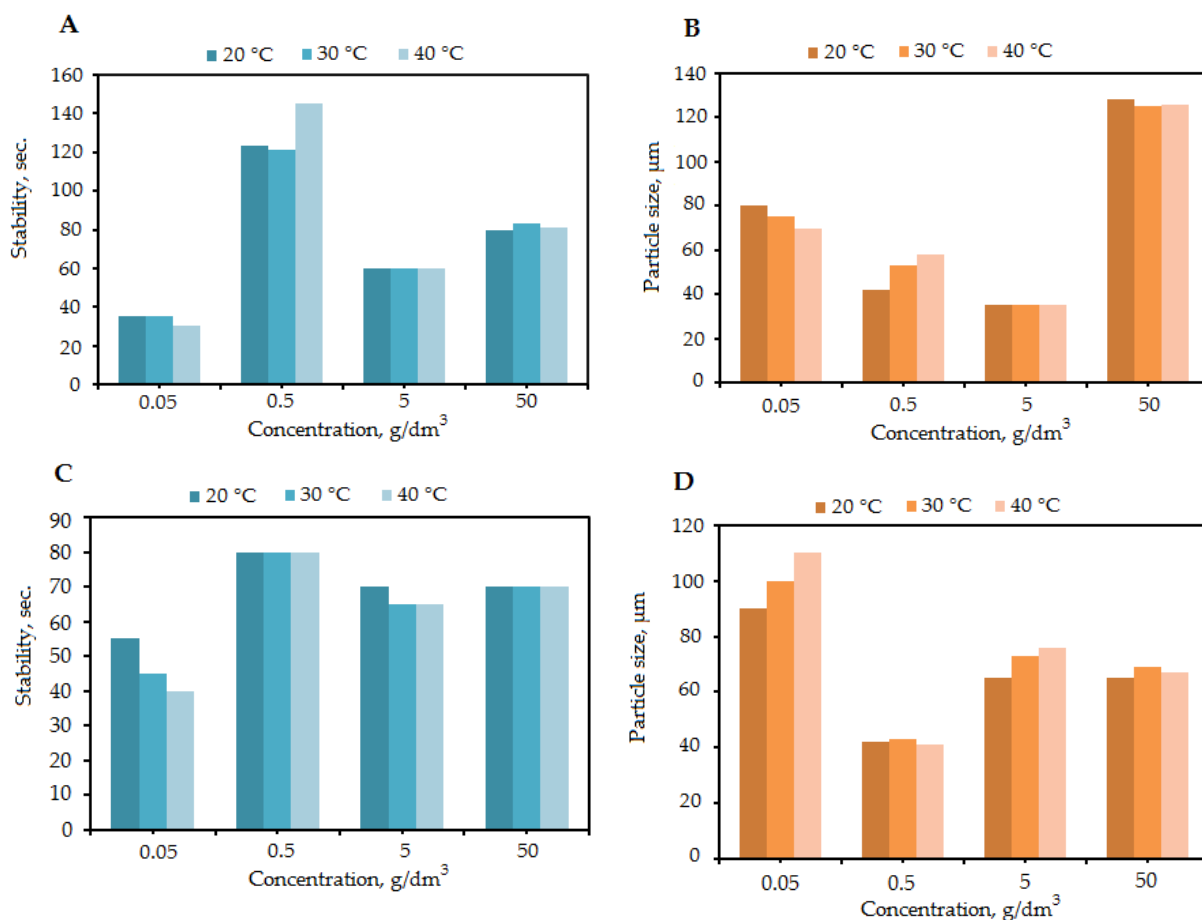


Figure 5. Influence of frother solution concentration on stability and size of WAME: (A,B)—reagent T-92; (C,D)—reagent BTF-163.

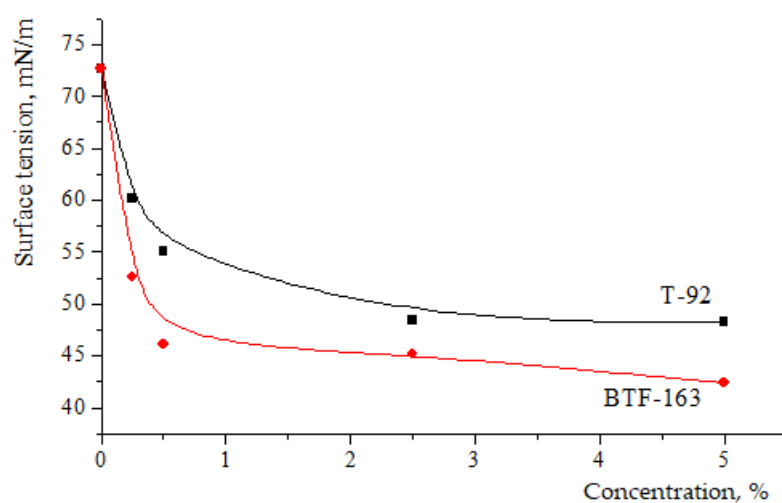
The oxal T-92 reagent produced a stable microemulsion at a concentration of 0.5 g/dm³ (121–145 s) with a size of 42–58 µm. A water-air microemulsion with 35–40 microns size was obtained at a concentration of 5 g/dm³. BTF-163 produced a stable microemulsion at a concentration of 0.5 g/dm³: the stability was 80 s, and the microemulsion size was 41–43 microns.

The surface tension of the reagent solution affects stability and microbubble size. T-92 produced stable microbubbles at a concentration of 5 g/dm³ and a surface tension value of $\sigma = 48.4$ mN/m. BTF-163 produced stable microbubbles at a concentration of 0.5 g/dm³ and a surface tension value of $\sigma = 42.4$ mN/m [21]. Table 5 shows the size of the WAME and the electrokinetic potential of the reagent solution.

Table 5. The size of WAME and the electrokinetic potential of reagent solution.

Name of Reagents	Bubble Size, μm	Electrokinetic Potential, mV
T-92—0.25% (2.5 mg/dm ³)	120 (63.4%)	−6.65
T-92—0.5% (5 mg/dm ³)	62 (48.4%)	−8.1
T-92—2.5% (25 mg/dm ³)	27 (63.5%)	−6.9
BTΦ-163—0.5% (5 mg/dm ³)	39 (91.6%)	−11.4
BTΦ-163—2.5% (25 mg/dm ³)	22 (87.6%)	−11.8
BTΦ-163—5% (50 mg/dm ³)	20 (72.4%)	−8.1

The change in the surface tension of the reagent solutions as a function of concentration is shown in Figure 6.

**Figure 6.** Dependence of the surface tension of reagent solutions on concentration.

The surface tension of the T-92 solution was 55.1 mN/m, and that of the BTF-163 solution was 46.1 mN/m at a concentration of 0.5%. The lower the frother solution surface tension, the more stable the foam stability. Usually, the highest foam stability corresponds to the concentration of the reagent at which there is a sharp decrease in surface tension.

3.2. Results of Polymetallic Cu-Pb-Zn-Fe Ore Flotation

The results of copper-lead rougher flotation without and with the use WAME generator are presented in Table 6.

Table 6. Copper-lead flotation results in the basic mode and with the use of WAME generator.

Product Name	Yield, %	Content, %				Extraction, %				Note
		Cu	Pb	Zn	Fe	Cu	Pb	Zn	Fe	
Cu-Pb Concentrate	2.5	11.3	13.5	6.3	14.7	85.28	81.23	4.29	6.76	Basic mode (without generator)
Tailings	97.5	0.05	0.08	3.6	5.2	14.72	18.77	95.71	93.24	
Initial ore	100	0.33	0.42	3.67	5.44	100	100	100	100	
Cu-Pb Concentrate	2.7	11.1	12.9	7.2	16.2	88.3	85.6	5.4	7.8	With generator
Tailings	97.3	0.041	0.06	3.5	5.3	11.7	14.4	94.6	92.2	
Initial ore	100	0.34	0.41	3.6	5.59	100	100	100	100	

The copper-lead rougher concentrate was obtained at the optimum basic mode (Table 4), and contained 11.3% copper at 85.28% recovery, and 13.5% lead at 81.23% recovery. The copper-lead rougher concentrate with a copper content of 11.1% with 88.3% recovery, and lead 12.9% with 85.6% recovery was obtained using the air-water microemulsion generator. The application of the WAME generator allowed for the maintenance of the quality of the copper-lead rougher concentrate in terms of the copper and lead content and for the increase in copper extraction by 3.02% and lead extraction by 4.37%.

The copper-lead rougher concentrate with 11.1% copper content at 88.3% recovery and 12.9% lead content at 85.6% recovery was obtained with the use of the generator. The application of the WAME generator allowed for the maintenance of the quality of the copper-lead rougher concentrate in terms of the copper and lead content and for the increase in copper recovery by 3.02% and lead recovery by 4.37%.

3.3. Polymetallic Cu-Mo Ore Flotation Results

The enlarged laboratory tests result of the copper-molybdenum flotation cycle of copper-containing ore at the optimal basic mode and using the WAME generator are shown in Table 7.

Table 7. Copper-molybdenum rougher flotation results in the basic mode and with the WAME generator use.

Product Name	Yield, %	Content, %		Extraction, %		Note
		Cu	Mo	Cu	Mo	
Cu-Pb Concentrate	1.45	22.3	0.8	82.4	70.2	Basic mode (without generator)
Tailings	98.55	0.07	0.005	17.6	29.8	
Initial ore	100	0.39	0.017	100.0	100.0	
Cu-Pb Concentrate	1.57	22.1	0.75	87.6	74.9	With generator
Tailings	98.43	0.05	0.004	12.4	25.1	
Initial ore	100	0.40	0.016	100.0	100.0	

The copper-molybdenum rougher concentrate with 1.45% yield, containing 22.3% copper at 82.4% recovery and 0.8% molybdenum at 70.2% recovery were obtained in the basic mode. The copper-molybdenum rougher concentrate with 1.57% yield, containing 22.1% copper at 87.6% recovery and 0.75% molybdenum at 74.9% recovery was obtained with the WAME generator.

The test results show that using the WAME generator allowed for the maintenance of the quality of the copper-molybdenum concentrate and for the increase in the copper recovery by 5.2% and molybdenum recovery by 4.7%. Thus, using the WAME generator can improve the technological indicators of rougher flotations.

3.4. Gold-Bearing Ore Flotation Results

The test result of the laboratory experiments in the basic mode without and with a generator are presented in Table 8.

Table 8. Results of laboratory experiments in basic mode without and with a generator.

Product Name	Yield, %	Content, g/t	Extraction, %	Note
Intercycle flotation concentrate	15.43	7.70	70.58	Basic mode (without generator)
Au-bearing concentrate	0.85	25.63	13.01	
Total Concentrate	16.28	8.64	83.59	
Tailings	83.72	0.33	16.41	
Initial ore	100	1.68	100	
Intercycle flotation concentrate	14.14	9.21	75.71	Feeding reagents through the generator in all cycles (intercycle, rougher and scavenger flotation)
Au-bearing concentrate	0.82	20.95	9.95	
Total Concentrate	14.96	9.85	85.66	
Tailings	85.04	0.29	14.34	
Initial ore	100	1.72	100	
Intercycle flotation concentrate	11.17	14.14	80.94	Feeding reagents through the generator in the rougher and scavenger flotation cycles
Au-bearing concentrate	1.13	11.99	6.93	
Total Concentrate	12.30	13.94	87.86	
Tailings	87.70	0.27	12.14	
Initial ore	100	1.95	100	

The total concentrate yield compared to the basic mode decreased by 1.32% from 16.28% to 14.96%, the quality increased by 1.21 g/t (from 8.64 g/t to 9.85 g/t), and the recovery increased by 2.07% (from 83.59% to 85.66%) by using the WAME generator in all flotation cycles.

By using the WAME generator in the rougher and scavenger flotation cycles, indicators of flotation gold extraction were significantly improved in comparison with the basic mode. The concentrate quality increased by 5.3 g/t (from 8.64 g/t to 13.94 g/t), and extraction increased by 4.27% (from 83.59% to 87.86%).

By using a water-air microemulsion in a frother solution, the technological performance increase is associated with the frothing ability of the frother. The higher the reagent foaming ability, the larger the obtained water-air microemulsion volume is.

The concentrate yield, grade, and recovery—these three parameters need to be adjusted correctly in the flotation. If the foam product yield increases, the useful component content may decrease, and the recovery may increase. It is necessary to find the optimal parameters. In the case of the application of microbubbles, the parameters depend on the ratio of microbubbles to useful mineral microparticles. It is assumed that for one valuable mineral particle with a size of less than 30 microns, the optimal number of microbubbles should be about 8–10 microbubbles.

Insufficient and excessive amounts of microbubbles negatively affect the flotation process. An insufficient amount will not allow for the complete extraction of fine useful minerals; an excessive amount worsens the froth product quality. The optimal amount can be adjusted by increasing or decreasing the frother flow. For example, in this study of polymetallic ore flotation, the frother amount did not change. In the gold-bearing ore flotation, the T-92 amount decreased by half.

3.5. Frother Solutions Foaming Ability

Figure 7 shows the foaming ability of reagents T-92 and BTF-163 at different concentrations: 0.05%; 0.1%; and 0.5%.

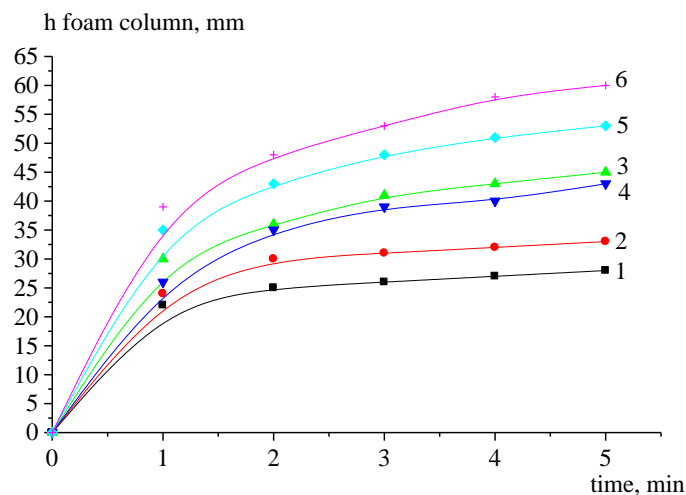


Figure 7. Foaming ability of T-92 (1,2,3) and BTF-163 (4,5,6) at different concentrations: (1) $C = 0.05\%$ (0.5 g/dm^3); (2) $C = 0.5\%$ (5 g/dm^3); (3) $C = 5\%$ (50 g/dm^3); (4) $C = 0.05\%$ (0.5 g/dm^3); (5) $C = 0.5\%$ (5 g/dm^3); (6) $C = 5\%$ (50 g/dm^3).

The foaming ability increases with increasing concentration. This is due to micelle formation, as when the critical concentration of micelle formation (CCM) is reached, the maximum foam volume is observed. The adsorption layer with the maximum mechanical strength is formed in the CCM region. The reagent foaming ability depends on the reagent composition [22]. The diffusion rate of the molecules into the surface layer decreases with a further increase in the frother solution concentration (above the CCM). This explains some of the decrease in the foaming ability [23,24].

The foam stability decreases if the sizes of the bubbles in contact with each other are significantly different. This is explained by the fact that there is a large difference in capillary pressures between bubbles of different sizes. Compounds containing one of the polar groups, $-\text{OH}$, $=\text{COOH}$, $=\text{C}=\text{O}$, $-\text{NH}_2$, $-\text{SO}_2\text{OH}$, or $-\text{HSO}_3$, in their composition are the most effective.

The foam stability is also affected by the reagent structure. The frother surface activity depends on the hydrophilic–lipophilic balance, i.e., on the polar and non-polar group ratio. Reagent T-92 is a mixture of aliphatic alcohols, esters, and organic acids. Non-polar groups have short radicals, so polar groups such as OH^- , COO^- , etc., prevail. BTF-163 is a phosphorus-containing sulfhydryl flotation agent. It has a more branched structure with two long radicals and one sulfhydryl polar group, has both collecting and foaming ability, and has more pronounced surface activity. Therefore, the T-92 is less active than the BTF-163.

4. Conclusions

1. Theoxal T-92 reagent produces a stable microemulsion at a concentration of 5 g/dm^3 . BTF-163 produces a stable microemulsion at a concentration of 0.5 g/dm^3 .
2. The copper-lead concentrate quality was maintained in terms of copper and lead content, copper extraction increased by 3.02%, and lead extraction increased by 4.37% when using the generator in the Cu-Pb rougher flotation cycle during Cu-Pb-Zn-Fe ore processing.
3. The copper-molybdenum concentrate quality was maintained, copper recovery increased by 5.2%, and molybdenum recovery increased by 4.7% when using the generator in the Cu-Mo rougher flotation cycle during Cu-Mo ore processing.

4. The flotation extraction indicators of gold in the concentrate were improved in comparison with the basic mode when using the generator in the rougher and scavenger flotation cycles. The gold content in the concentrate increased by 5.3 g/t and extraction increased by 4.27%.

Author Contributions: Conceptualization, D.T.; methodology, D.T. and N.T.; investigation, D.T., N.T., S.N. and Z.K.; data curation, D.T.; writing—original draft preparation, D.T. and N.T.; writing—review and editing, D.T. and S.N.; visualization, D.T. and N.T.; project administration, D.T. All authors have read and agreed to the published version of the manuscript.

Funding: This research was funded by the Ministry of Education and Science of the Republic of Kazakhstan (Project AP08856041).

Institutional Review Board Statement: Not applicable.

Informed Consent Statement: Not applicable.

Data Availability Statement: Not applicable.

Acknowledgments: The authors acknowledge the funding support from the Ministry of Education and Science of the Republic of Kazakhstan.

Conflicts of Interest: The authors declare no conflict of interest.

References

1. Li, M.; Liu, J.; Li, J.; Xiang, B.; Manica, R.; Liu, Q. Enhancement of selective fine particle flotation by microbubbles generated through hydrodynamic cavitation. *Powder Technol.* **2022**, *405*, 117502. [[CrossRef](#)]
2. Wang, D.; Liu, Q. Hydrodynamics of froth flotation and its effects on fine and ultrafine mineral particle flotation: A literature review. *Miner. Eng.* **2021**, *173*, 107220. [[CrossRef](#)]
3. Glembotsky, A.V. Flotation of ultrafine particles. *Non-Ferr. Met.* **1978**, *7*, 112–114.
4. Sebba, F. An improved generator for micron-sized bubbles. *Chem. Ind.* **1985**, *4*, 91–92.
5. Bocharov, V.A.; Vigderhaus, V.E. Flotation of sulfide fine mineral systems. *Non-Ferr. Met.* **1997**, *3*, 8–11.
6. Zagainov, V.G. Development of a method of flotation with ejector aeration with separation of gases from the liquid phase. *Ind. Kazakhstan* **2007**, *2*, 58.
7. Mukhanova, A.A.; Yessengazyev, A.M.; Barmenshinova, M.B.; Samenova, N.O.; Toilanbay, G.A.; Toktagulova, K.N. Improvement of the technology related gold-containing raw materials with the use of ultramicroheterogeneous flotoreagent. *Metalurgija* **2022**, *61*, 777–780. Available online: <https://hrcak.srce.hr/file/397152> (accessed on 1 July 2022).
8. Rulyov, N.N.; Filippov, L.O.; Kravchenko, O.V. Combined microflotation of glass beads. *Colloids Surf. A Physicochem. Eng. Asp.* **2020**, *598*, 124810. [[CrossRef](#)]
9. Farrokhpay, S.; Filippova, I.; Filippov, L.; Picarra, A.; Rulyov, N.; Fornasiero, D. Flotation of fine particles in the presence of combined microbubbles and conventional bubbles. *Miner. Eng.* **2020**, *155*, 106439. [[CrossRef](#)]
10. Rulyov, N.; Filippov, L.; Sadovskiy, D.; Lukianova, V. Reverse Combined Microflotation of Fine Magnetite from a Mixture with Glass Beads. *Minerals* **2020**, *10*, 1078. [[CrossRef](#)]
11. Rulyov, N.N.; Tussupbayev, N.K.; Turusbekov, D.K.; Semushkina, L.V.; Kaldybaeva, Z. Effect of microbubbles as flotation carriers on fine sulphide ore beneficiation. *Miner. Process. Extr. Metall.* **2018**, *127*, 133–139. [[CrossRef](#)]
12. Zhang, Z.; Ren, L.; Zhang, Y.; Bao, S. Microflotation of Fine Rutile and Garnet with Different Particle Size Fractions. *Minerals* **2022**, *12*, 1238. [[CrossRef](#)]
13. Li, H.; Afacan, A.; Liu, Q.; Xu, Z. Study interactions between fine particles and micron size bubbles generated by hydrodynamic cavitation. *Miner. Eng.* **2015**, *84*, 106–115. [[CrossRef](#)]
14. Wang, Q.; Chen, Y.; Huang, J.; Gao, B.; Chen, Y. Research on Application of Hydrocyclone Microbubbles Generator in Flotation of Oil-Water Emulsion. *J. Phys. Conf. Ser.* **2021**, *2076*, 012080. [[CrossRef](#)]
15. Zhang, Z.; Ren, L.; Zhang, Y. Role of nanobubbles in the flotation of fine rutile particles. *Miner. Eng.* **2021**, *172*, 107140. [[CrossRef](#)]
16. Rahman, A.; Ahmad Kh Mahmoud, A.; Maoming, F. Nano-microbubble flotation of fine and ultrafine chalcopyrite particles. *Int. J. Min. Sci. Technol.* **2014**, *24*, 559–566. [[CrossRef](#)]
17. Rulyov, N.N. Turbulent microflotation: Theory and Experiment. *Colloids Surf. A Physicochem. Eng. Asp.* **2001**, *192*, 73–91. [[CrossRef](#)]
18. Rulyov, N.N. Turbulent microflotation of ultra-fine minerals. *Miner. Process. Extr. Metall.* **2008**, *117*, 32–37. [[CrossRef](#)]
19. Turysbekov, D.; Tussupbayev, N.; Semushkina, L.; Narbekova, S.; Kaldybaeva, Z.; Mukhamedilova, A. Study of the properties of water-air microdispersion of a floatation agent solution. *Metalurgija* **2022**, *61*, 363–366. Available online: <https://hrcak.srce.hr/file/386165> (accessed on 1 April 2022).

20. Turysbekov, D.K.; Tusspbayev, N.K.; Semushkina, L.V.; Narbekova, S.M.; Mukhamedilova, A.M. Determination of factors affecting properties of water-air microdispersion. *Complex Use Miner. Resour.* **2022**, *322*, 5–13. [[CrossRef](#)]
21. Turysbekov, D.; Tussupbayev, N.; Semushkina, L.; Narbekova, S.; Kaldybaeva, Z.; Mambetaliyeva, A. Effect of the water-air emulsion size of the foaming agent solution on the non-ferrous metal minerals flotation ability. *Metalurgija* **2021**, *60*, 395–398. Available online: <https://hrcak.srce.hr/file/372284> (accessed on 1 July 2021).
22. Tikhomirov, V.K. Foams. Theory and Practice of Obtaining and Destruction. 1983. Available online: <https://bookree.org/reader?file=476284> (accessed on 1 April 2022).
23. Semushkina, L.V.; Tusupbaev, N.K.; Shautenov, M.R.; Suleimenova, U.Y.; Kalieva, R.S.; Onaev, M.I. Study of foam-forming ability of a new flotation agent of tetrahydropyrane series. *Bull. Kazakh Natl. Tech. Univ.* **2008**, *5*, 152–156.
24. Drzymala, J.; Kowalczyk, P. Classification of Flotation Frothers. *Minerals* **2018**, *8*, 53. [[CrossRef](#)]